Desalination and Water Treatment
www.deswater.com

doi: 10.5004/dwt.2017.21206

84 (2017) 262–270
July

Potassium hydroxide-treated palm kernel shell sorbents for the efficient removal of methyl violet dye

See Ming-Twang[a], Muhammad Abbas Ahmad Zaini[a,b,*], Liza Md. Salleh[a,b], Mohd. Azizi Che Yunus[a,b], Mu. Naushad[c]

[a]*Department of Chemical Engineering, Faculty of Chemical and Energy Engineering, Universiti Teknologi Malaysia, 81310 UTM Johor Bahru, Malaysia, emails: abbas@cheme.utm.my (M.A.A. Zaini), geminitwang@hotmail.com (S. Ming-Twang), i.liza@cheme.utm.my (L.M. Salleh), r-azizi@utm.my (M.A.C. Yunus)*
[b]*Centre of Lipids Engineering and Applied Research (CLEAR), Ibnu-Sina Institute for Scientific and Industrial Research (ISI-SIR), Universiti Teknologi Malaysia, 81310 UTM Johor Bahru, Malaysia*
[c]*Advanced Materials Research Chair, Department of Chemistry, College of Science, Building #5, King Saud University, Riyadh 11451, Saudi Arabia, email: mnaushad@ksu.edu.sa (M. Naushad)*

Received 19 January 2017; Accepted 12 July 2017

ABSTRACT

The present work was aimed to evaluate the removal of methyl violet dye by potassium hydroxide-treated palm kernel shell sorbents. The sorbents were prepared by dried impregnation, carbonization and chemical activation in a muffle furnace. The sorbents were characterized for specific surface area, surface morphology and functional groups. Results show that the activated carbon displayed a specific surface area of 302 m^2/g, which was 54 times greater than the impregnated sorbent. However, the latter showed a 42 mg/g maximum adsorption capacity of methyl violet, nearly four times better than the former. The equilibrium data were fitted well with the Langmuir isotherm, while the rate of sorption data obeyed the pseudo-second-order model. Adsorption of methyl violet was not specific surface area-dependent. The rate-limiting step for methyl violet adsorption was mainly driven by film diffusion at lower concentration, and intraparticle diffusion at higher concentration. A simple impregnation using potassium hydroxide was a promising approach to yield sorbent rich in acidic groups for methyl violet removal.

Keywords: Adsorption; Dried impregnation; Methyl violet dye; Palm kernel shell; Potassium hydroxide

1. Introduction

Water pollution due to industrial and agricultural activities has become the challenging threat to human being. Regardless in developing or non-developing countries, groundwater for daily life is excessively polluted with toxic pollutants like anions, heavy metals, organic compounds and dyes [1–5]. Dyes in water are originated from textiles, papermaking, printing, colouring, food processing and cosmetic industries. Over 700,000 tons of wastewater produced every year is due to dyes [6,7]. Methyl violet is an example of the commonly used basic dyes with high colour intensity. The presence of dyes in water prevents the sunlight from penetrating into the stream, thus hindering the aquatic plants to carry out photosynthesis. Moreover, prolonged exposure to dyes beyond the concentration limits can cause harm to aquatic creatures and lead to severe health problems to human via the food chain [8].

Various methods have been projected for the removal of dyes from aqueous medium like coagulation [9], advance oxidation [10], membrane filtration [11], photocatalysis [12,13], capillary electrophoresis [14], spectrophotometric method [15,16], adsorption [17,18] and liquid chromatography method [19,20]. In general, most of these methods are

* Corresponding author.

not sustainable because of the production of sludge that requires special handling and disposal. In addition, the equipment and facilities involved incur high capital, operating and maintenance costs. Adsorption by activated carbon has been a preferable method for dye removal because of the stability and efficiency of sorbent, and the simplicity in the process, design and scale-up [21]. However, the commercial activated carbon is expensive because it is mainly derived from non-renewable materials. Moreover, the regeneration of spent sorbent is difficult and often yields poor performance for successive use. Therefore, the quest for abundantly available precursors mainly from agricultural by-products has become a topic of considerable interest to sustain the use of sorbent for dyes removal. A promising candidate under this category is palm kernel shell [22,23].

Palm kernel shell-based sorbents can be prepared through impregnation, carbonization, simple chemical treatment, and physical and/or chemical activation, and have been extensively studied for different types of model pollutants [22–27]. It should be noted that, water pollutants normally exhibit dissimilar selectivity and affinity of removal by adsorbents [22,23]. This is particularly due to the nature of the precursor and the physicochemical properties of adsorbate. Hence, it is a challenging task to synthesize the sorbent that performs well for a specific water pollutant. To narrow down the gap in the body of knowledge, the present work was aimed at evaluating three sorbents derived from palm kernel shell, namely activated carbon, impregnated sorbent and char for methyl violet dye removal. Potassium hydroxide was used as the oxidizing agent. Thermal treatment was carried out using a muffle furnace and microwave treatment. Isotherm and kinetics models were used to describe the adsorption data. The results and findings were discussed and compared with the present literature.

2. Materials and methods

2.1. Materials

Raw palm kernel shell was obtained from a palm oil mill factory located in the Johor state of Malaysia. The model dye, methyl violet ($C_{24}H_{28}N_3Cl$, 393.95 g/mol, C.I. 42535, λ_{max} = 586 nm) was purchased from R&M Marketing, UK. All chemicals used were of analytical grade reagents.

2.2. Preparation of sorbents

Three sorbents were derived from palm kernel shells. Palm kernel shell (average size of 1.3 cm) was mixed with potassium hydroxide solution at a mass ratio (reagent to precursor) of 0.5. The dried impregnated sample was heated in a furnace for activation at 550°C for 1.5 h, and the resultant activated carbon was denoted as FS. The mixture of palm kernel shell in potassium hydroxide solution (solid mass ratio of 0.5) was dried in microwave oven at 70% power intensity for 0.5 h, and the impregnated sorbent was designated as MS. The third sorbent was prepared by heating the palm kernel shell in furnace at 250°C for 1.5 h. The char produced was labelled as CS. All sorbents were soaked in 3 M of HCl overnight to remove surface impurities, followed by subsequent washing with hot distilled water to a constant pH. The sorbents were dried in oven at 110°C prior to use.

2.3. Samples characterization

Field emission scanning electron microscope (FESEM, SUPRA 35VP) was used to evaluate the surface morphology of sorbents. This instrument is equipped with energy dispersive X-ray for the measurement of surface composition of carbon and oxygen. The single point specific surface area was obtained by using a Pulse Chemi Sorb 2705 analyzer. Surface chemistry of sorbents was determined using Fourier transform infrared instrument (FTIR, Spectrum One). Boehm titration was carried out to measure the concentration of acidic oxygen functional groups. Briefly, 300 mg of each sorbent was brought into contact with 15 mL of 0.1 M sodium hydroxide solution. The mixture was placed in an orbital shaker at 120 rpm and room temperature for 48 h. The concentration of acidic groups was determined by back-titrating 5 mL of each aliquot with 0.05 M HCl. Phenolphthalein was used as an indicator for the neutralization end-point of the titration.

2.4. Adsorption studies

Batch adsorption was carried out by adding 0.05 g of each sorbent in 50 mL of methyl violet solution of varying concentrations (2–100 mg/L). The solution pH was not adjusted, and was measured as 4.93 ± 0.23. The mixtures were placed in an orbital shaker at 120 rpm and room temperature for 72 h. The residual concentrations were measured using a visible spectrophotometer (Libra S6) at a wavelength of 485 nm. The calibration was established as a.u. = 0.0388 × concentration, R^2 = 0.994 for methyl violet concentrations between 0 and 15 mg/L. The adsorption capacity was calculated as $Q_e = (C_o - C_e) \times V/m$, where C_o and C_e (mg/L) are the initial and equilibrium concentrations, respectively, V (L) is the volume of solution and m (g) is the mass of sorbent.

The sorbent that displayed appreciable methyl violet removal was evaluated for the rate of adsorption. Two concentrations were selected on the basis of equilibrium adsorption, that is, concentrations that demonstrate strong affinity and maximum capacity. Fifty milligrams of sorbent was added into 50 mL of methyl violet solution in different batches with concentrations of 10 and 60 mg/L. At different time intervals for 72 h, the supernatant was withdrawn, and the residual concentration of methyl violet was measured using visible spectrophotometer. The adsorption of methyl violet at time t, was calculated as $Q_t = (C_o - C_t) \times V/m$, where C_t (mg/L) is the concentration of dye at time t.

3. Results and discussion

3.1. Characteristics of sorbents

The raw palm kernel shell used in this work contained 12% moisture and 1.3% ash, and had a specific surface area of 2.76 m^2/g. The characteristics of sorbents derived from palm kernel shell are summarized in Table 1.

The yield of FS is lower compared with the other two sorbents because of the dehydrating effect of potassium hydroxide during the activation at high temperature. The process is expected to initiate the bond cleavage of weakly connected bridges in the impregnated material, leading to the release volatile products and consequently weight loss due to the oxidation reactions [21]. The liberation of volatiles

also creates more pathways and channels that bring about a higher surface area of FS. The excessive removal of volatiles also yields a rich carbon content of FS. On the other hand, MS exhibits a 40% yield, by which the weight loss is likely due to the use of oxidizing agent. The specific surface area of MS is not well-developed, while the rich oxygen content could be associated with the abundance of acidic oxygen functional groups.

Surface morphology can assist in identifying the surface structure and pore arrangement of the sorbent. Fig. 1 shows the surface morphology of palm kernel shell and the derived sorbents. The palm kernel shell exhibits a rough surface of undeveloped pores as compared with FS. Cracks and crevices in the range of 1–2 μm were observed on the surface of the derived sorbents. FS exhibits a well-developed porous texture with honeycomb-like structure. On the contrary, CS displays a surface with large holes and rudimentary pores that explains its lower specific surface area than palm kernel shell. The SEM images are in agreement with the specific surface area data shown in Table 1. FS shows a specific surface area of 302 m^2/g that is about 54 times higher than MS. A higher surface area generally offers greater interaction probabilities between sorbent surface and pollutant molecules for a better adsorption.

Surface functional groups could play a considerable role in the adsorption of water pollutants through ion-exchange, π interactions and formation of complexes [21,28,29]. The FTIR spectra of sorbents are shown in Fig. 2, and the possible functional groups are listed in Table 2. From Fig. 2(a), it is obvious that a number of important surface functional groups diminished after chemical activation as illustrated in the FS spectrum. This could be due to the dual effects of dehydrating agent (potassium hydroxide) at high temperature that accelerates the liberation of volatiles. On the other hand, MS shows more peaks associated with the surface acidic functional groups compared with palm kernel shell and CS. The difference in peaks intensities can be seen in Fig. 2(b). This could be attributed to the oxidation of carbon

Table 1
Characteristics of sorbents

Sorbent	Yield (wt%)	Carbon content (wt%)	Oxygen content (wt%)	Specific surface area (m^2/g)	pH	Acidic groups (mmol/g)
CS	76.3	65	35	1.73	5.2	0.533
MS	40.1	57	43	5.63	4.6	1.04
FS	19.8	87	13	302	4.9	0.467

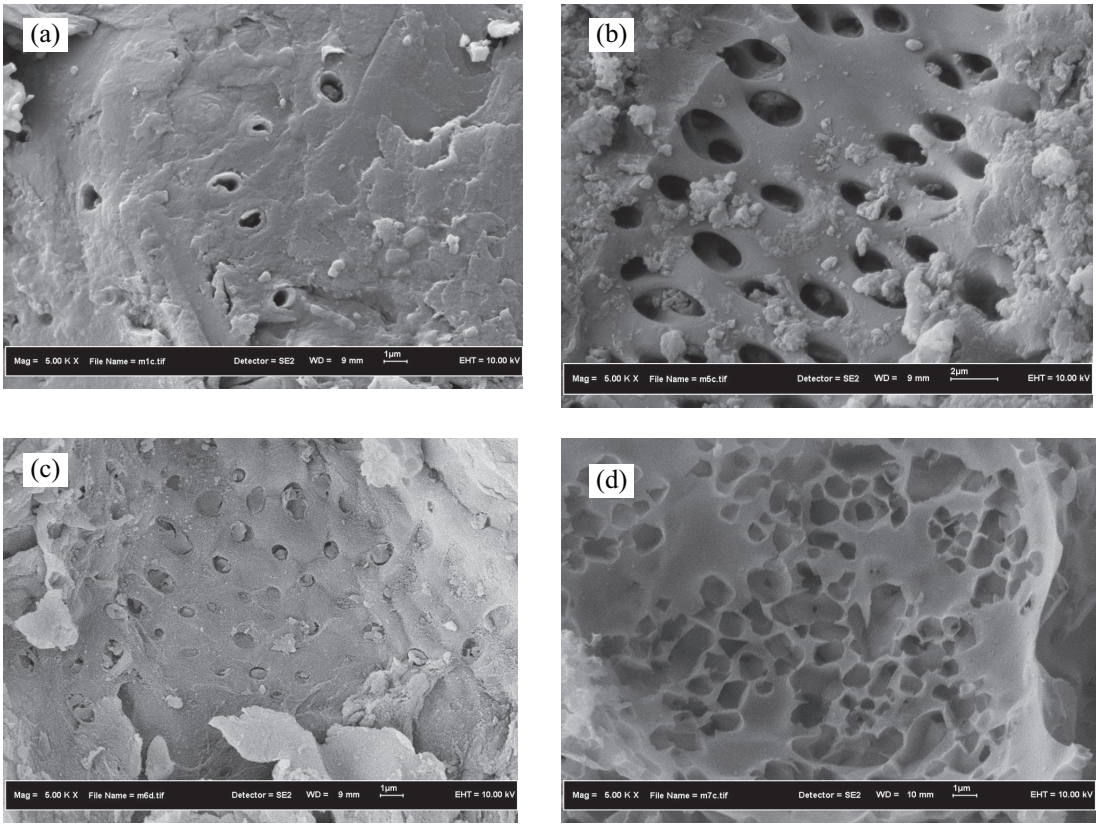

Fig. 1. SEM images of (a) palm kernel shell, (b) char (CS), (c) impregnated sorbent (MS) and (d) activated carbon (FS).

surface by potassium hydroxide (oxidizing agent) at mild temperature. It was found that, the use of hydroxide salt in this work has enhanced the development of oxygen containing functional groups on the surface of MS upon impregnation (Table 1). The existence of oxygen functional groups on the sorbent surface is likely to promote better adsorption of some water pollutants [23,30].

In general, palm kernel shell, MS and CS demonstrate a similar pattern of the FTIR spectra. For the sorbents studied, the overlay view of MS and CS spectra is shown in Fig. 2(b). Obviously, the intensity of surface functional groups in MS is higher than that in CS, especially that of O–H stretch, C=O stretch as well as C–O–C stretch bands. From the viewpoint of surface chemistry, it can be reasonably predicted that MS possesses a stronger affinity for adsorption of certain types of pollutants due to rich acidic oxygen functional groups, such as carboxylic (OH–C=O), lactonic (C=O) and phenolic (C–OH) [30,31]. This is supported by the quantitative measurement of Boehm titration as presented in Table 1, and the assignment of surface functional groups from FTIR spectra in Table 2.

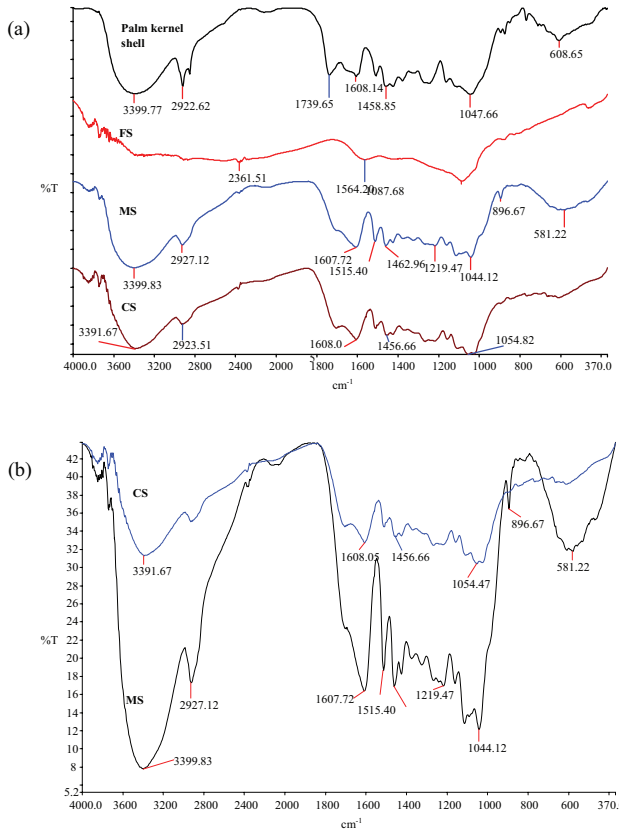

Fig. 2. (a) FTIR spectra of palm kernel shell and the derived sorbents (split view) and (b) FTIR spectra of CS and MS (overlay view).

3.2. Equilibrium adsorption of methyl violet

Adsorption of methyl violet was carried out to evaluate the performance of palm kernel shell-based sorbents. Fig. 3 shows the effect of concentration on the removal capacity of methyl violet sorbents.

In general, the removal capacity of methyl violet increased with increasing concentration because the concentration gradient acts as a driving force in alleviating the mass transfer resistance between aqueous phase and solid phase. This is true if the active sites are still vacant to accommodate the methyl violet molecules, to a saturation point when the adsorption capacity reaches the maximum value. From Fig. 3, the adsorption of methyl violet is in the order of MS > FS > CS. At initial concentration of 20 mg/L, MS recorded a 17 mg/g of methyl violet removal, compared with 11 and 3 mg/g by FS and CS, respectively. A higher methyl violet removal by MS could be attributed to the sorbent surface chemistry that is

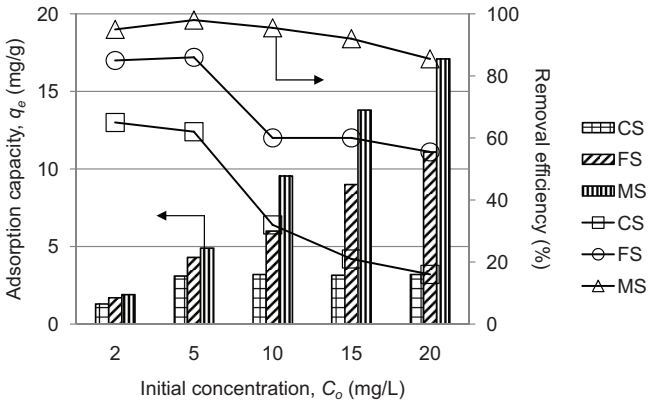

Fig. 3. Effect of initial concentration on the removal of methyl violet by palm kernel shell sorbents.

Table 2
Infrared assignment and surface functional groups

Absorption band (cm^{-1})				Assignment	Functional groups
Palm kernel shell	FS	MS	CS		
3,400	–	3,400	3,392	O–H stretch	Hydroxyl, phenolic
2,923	–	2,927	2,924	C–H stretch	Methylene
1,740–1,068	1,564	1,608	1,608	C=O stretch	Quinone, carboxylic anhydrides
	–	1,515	–	C=C–C stretch	Aromatic ring
1,459	–	1,463	1,457	C–H bend	Methyl (CH_3)
1,048	1,088	1,219–1,044	1,055	C–O–C stretch	Ether
–	–	897	–	C–OH out of plane	Ether

rich in acidic oxygen functional groups. In solution, the rich acidic oxygen groups tend to release protons, rendering the negatively charged sorbent surface [30]. Consequently, the solution pH bearing MS slightly decreased upon equilibrium (pH_e = 4.3). Methyl violet is a basic dye that carries positive charge. As a result, the cationic dye molecules could lodge on the MS surface through electrostatic attraction, coordination mechanism and formation of complexes [11,12]. As for the removal efficiency, MS demonstrated a small decrease from 98% to 86% for the concentration range studied. A drastic drop in adsorption efficiency with increasing concentration reflects the unsuitability of the sorbent to be used at higher dye concentration.

Equilibrium adsorption is the state at any concentrations where the rate of adsorption is equal to the rate of desorption. Fig. 4 displays the equilibrium curves of methyl violet adsorption onto palm kernel shell-based sorbents.

All sorbents exhibit a similar pattern of increasing adsorption capacity with increasing equilibrium concentration, and the curves start to level off at different maximum values, that is, 42, 11 and 3.2 mg/g for MS, FS and CS, respectively. The concave upward trend of the equilibrium curves suggested that the adsorption of methyl violet is favourable onto palm kernel shell-based sorbents [22,23]. FS shows a greater methyl violet removal than CS. It signifies a positive effect of specific surface area of FS to promote adsorption of dye molecules. Poor performance of CS could be related to its lack of textural and surface properties for dye adsorption. The maximum removal of MS is nearly four times better than that of FS, even though the latter possesses surface area 54 times greater than the former. It is suggested that the removal of methyl violet is not sorbent surface area-dependent. In this work, surface chemistry of MS plays a dominating role on the removal of methyl violet, although the sorbent surface area is inferior. Similar findings using different model dyes and sorbent precursors are also reported elsewhere [29,31,32].

Three isotherm models, namely Langmuir, Freundlich and Redlich–Peterson were used to describe the equilibrium data of methyl violet sorbents [29,30]. The Langmuir isotherm explains the monolayer adsorption onto homogeneous sorbent surface, and is expressed as:

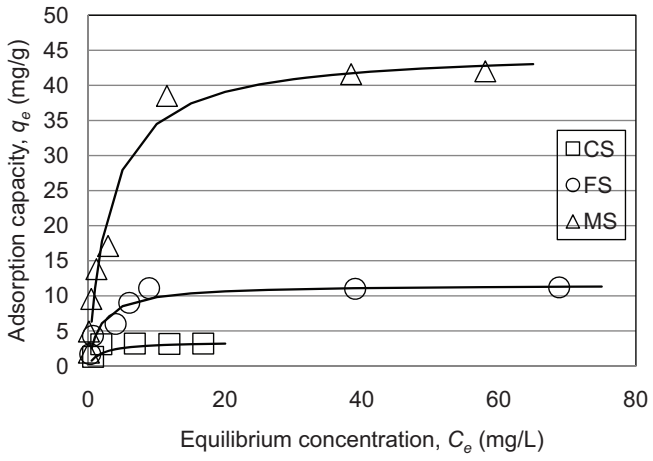

Fig. 4. Equilibrium adsorption of methyl violet by palm kernel shell sorbents (lines were predicted by Langmuir model).

$$q_e = \frac{Q_m b C_e}{1 + b C_e} \tag{1}$$

where Q_m (mg/g) is the maximum capacity to form monolayer of adsorbate on the sorbent surface, and b (L/mg) is a constant related to the affinity of binding sites. The empirical Freundlich isotherm is based on the adsorption onto heterogeneous surface, and is expressed as:

$$q_e = K C_e^{\frac{1}{n}} \tag{2}$$

where K and $1/n$ are the Freundlich constants related to the maximum adsorption capacity and intensity, respectively. The Redlich–Peterson model is a hybrid isotherm that combines both features of Langmuir and Freundlich equations, and is expressed as:

$$q_e = \frac{A C_e}{1 + B C_e^g} \tag{3}$$

where A, B and g are the Redlich–Peterson constants, and $0 < g < 1$. All isotherm constants, as summarized in Table 3 were solved using *Solver* add-in of MS Excel, given the condition where the sum of squared error (SSE) is the least, rendering optimum correlation of determination (R^2).

The applicability of the isotherm model to represent the adsorption data is judged based on the closeness of R^2 to unity and the smallest SSE. From Table 3, the adsorption data

Table 3
Constants of isotherm models

	CS	FS	MS
pH_e	4.9 ± 0.3	4.7 ± 0.3	4.3 ± 0.4
Langmuir model			
Q_m (mg/g)	3.48	11.6	45.1
b (L/mg)	1.40	0.555	0.327
SSE	0.543	7.24	60.2
R^2	0.811	0.918	0.976
Freundlich model			
K (mg/g)(L/mg)$^{1/n}$	2.12	5.13	13.6
n	5.81	4.73	3.30
SSE	1.15	19.0	152
R^2	0.588	0.786	0.927
Redlich–Peterson model			
A (L/g)	4.88	7.11	14.7
B	1.40	0.660	0.327
g	1.0	0.981	1.0
SSE	0.543	7.19	60.2
R^2	0.811	0.918	0.976

obeyed the Langmuir and Redlich–Peterson models. The g values equal or are close to unity indicate that the Redlich–Peterson model has been simplified into the Langmuir model [29,30]. Hence, it is postulated that the adsorption of methyl violet occurs on the homogeneous surface of palm kernel shell-based sorbents, and that it is monolayer in nature. Saeid et al. [33] reported the applicability of Langmuir model to describe the methyl violet adsorption onto granular FS with maximum monolayer adsorption of 95 mg/g.

From Table 3, the predicted Q_m agreed well with the maximum capacity obtained from the experiment (Fig. 4). However, the Langmuir constant b was found to be in the opposite order of CS > FS > MS. It denotes the pattern of energy for adsorption possessed by the monolayer surface to hold the adsorbate. It is suggested that CS, despite having a lower removal capacity, possesses a higher affinity for methyl violet at lower concentrations (<5 mg/L) [30].

3.3. Adsorption kinetics of methyl violet

Adsorption kinetics is essential in monitoring the efficiency of the process, equilibrium time and adsorption rate. MS was selected for adsorption kinetics at two methyl violet concentrations of 10 mg/L (strong affinity) and 60 mg/L (maximum capacity). Fig. 5 shows the effect of time on the removal of methyl violet by MS.

There is a sharp increase in methyl violet adsorption in the first 9 h, followed by subsequent slower uptake upon approaching equilibrium at 48 and 72 h for 10 and 60 mg/L, respectively. The reported values of contact time to attain equilibrium are in agreement with some of similar works using chemically treated effluent sludge sorbents for methylene blue removal [29,32,34]. The equilibrium capacity was measured as 9.6 and 42 mg/g, respectively (Fig. 4). The initial fast removal was due to a high concentration gradient [35,36] and unoccupied active sites on the sorbent surface. As the adsorbate molecules start to lodge on the active sites, the remaining molecules in the bulk solution become lesser thus decreasing the rate of adsorption ($dC_t/dt \to 0$).

Fig. 6 illustrates the estimated rate constant and adsorption order for methyl violet removal by MS. The expression of the adsorption rate for 10 and 60 mg/L can be deduced as rate = $0.258C_t^{1.8}$ and rate = $0.0355C_t^{2.1}$, respectively. It signifies that the methyl violet adsorption occurs at a faster rate at lower concentration, and attains the equilibrium much earlier. Depending on the availability of active sites, the sorbent can accommodate higher adsorbate concentration for higher removal capacity. However, the adsorption rate is likely to slow down due to inherent repulsion between neighbouring adsorbate molecules and competition for active sites. Because of that, a longer contact time would be required to achieve equilibrium.

The potential mechanisms and rate-controlling steps involved in the adsorption are evaluated using pseudo-first-order, pseudo-second-order and intraparticle diffusion models [29]. The pseudo-first-order model indicates that the external diffusion is a significant step, and is expressed as:

$$q_t = q_e\left(1 - e^{-k_1 t}\right) \tag{4}$$

where q_t (mg/g) is the amount of methyl violet adsorbed at time t (min), and k_1 (h^{-1}) is the rate constant of pseudo-first-order

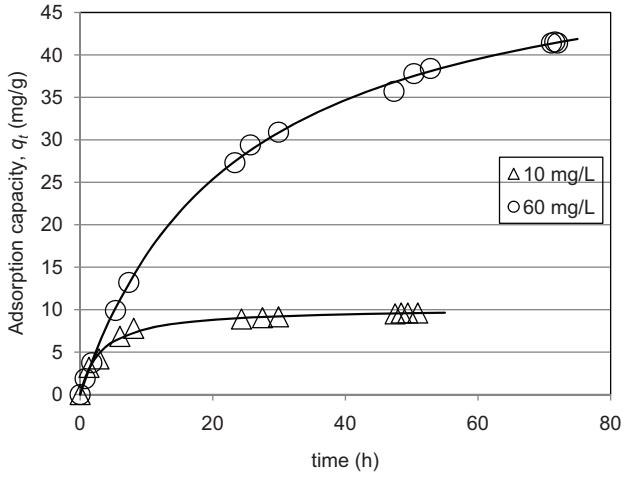

Fig. 5. Effect of time on methyl violet removal by MS (lines were predicted by pseudo-second-order model).

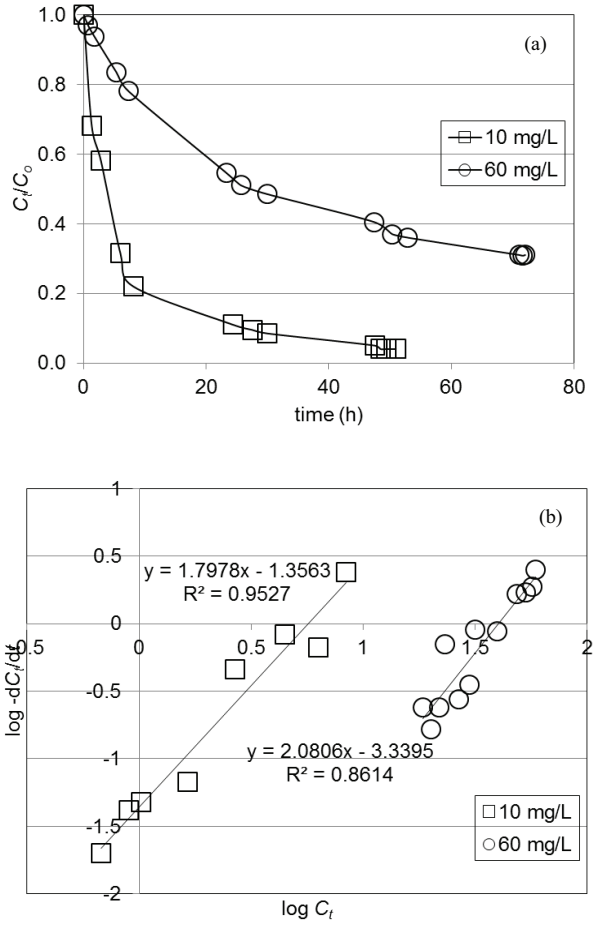

Fig. 6. (a) Changes of methyl violet concentrations against time. (b) Graphical approach for rate constant and adsorption order.

adsorption. The pseudo-second-order equation is based on chemical adsorption, and is expressed as:

$$q_t = \frac{k_2 q_e^2 t}{1 + k_2 q_e t} \tag{5}$$

where k_2 (g/mg h) is the rate constant of the pseudo-second-order adsorption. The initial adsorption rate, h (mg/g h) of the pseudo-second-order as $t \to 0$ is expressed as:

$$h = k_2 q_e^2 \tag{6}$$

The diffusion mechanism and rate-controlling steps in the adsorption process could be explained by the intraparticle diffusion model:

$$q_t = K_p t^{0.5} + C \tag{7}$$

where K_p (mg/g $h^{0.5}$) is the intraparticle diffusion rate constant, and C is the intercept that gives an idea about the boundary layer thickness, that is, the larger the intercept, the greater the boundary layer effect. All kinetics constants were solved using *Solver* add-in of MS Excel, and are summarized in Table 4.

Based on SSE and R^2 values, the adsorption rate of methyl violet onto MS could be described by the pseudo-second-order model, even though the model over predicted the values of equilibrium capacity. This is in accordance with the estimated adsorption order in Fig. 6. It is hypothesized that the adsorption of methyl violet by MS is chemisorption through sharing or exchange of electrons between active sites and dye molecules [29,32]. It is evident from the surface chemistry of MS that is rich in acidic oxygen functional groups. In a related development, Xu et al. [31] revealed that the adsorption of methyl violet occurs at acidic oxygen containing group such as –OH, –COO– and also C–O–C (1,065–1,045 cm^{-1}). Adsorption usually follows three consecutive steps, that is, (i) film diffusion which transports adsorbate molecules from bulk solution to the external surface of sorbent, (ii) particle diffusion which transports adsorbate molecules from liquid film to sorbent surface and (iii) adsorbate–sorbent interaction leading to adsorption.

Fig. 7 displays the intraparticle diffusion of methyl violet by MS at two different concentrations. The respective parameters are summarized in Table 3. From Fig. 7, there are two connecting lines of different slopes for adsorption using 10 mg/L methyl violet; the initial part indicates the initial stage of adsorption that reflects the thickness of boundary layer, and the second part represents the effect of intraparticle diffusion. As for 60 mg/L, the intraparticle diffusion could be the rate-limiting step as it yields a straight line through origin. At 60 mg/L, the film resistance is almost negligible because of thin boundary layer. However, it was not the case for 10 mg/L. Therefore, the intraparticle diffusion is not the only rate-limiting step that controlling the adsorption of methyl violet at lower concentration. Thus, the rate-limiting step for methyl violet onto MS is mainly driven by film diffusion at lower concentration, and thereafter switches to intraparticle diffusion as the film layer is suppressed as the concentration increases.

Table 4
Constants of kinetics models

	10 mg/L	60 mg/L
$q_{e,mea}$ (mg/g)	9.60	41.4
Pseudo-first-order model		
$q_{e,cal}$ (mg/g)	9.34	42.5
k_1 (h^{-1})	0.229	0.0449
SSE	1.14	7.65
R^2	0.990	0.998
Pseudo-second-order model		
$q_{e,cal}$ (mg/g)	10.2	54.9
k_2 (g/mg h)	0.0309	0.000781
h (mg/g h)	3.21	2.35
SSE	0.699	1.93
R^2	0.994	0.999
Intraparticle diffusion model		
K_p (mg/g $h^{0.5}$)	1.13	5.14
C (mg/g)	2.42	0
SSE	17.6	61.0
R^2	0.840	0.982

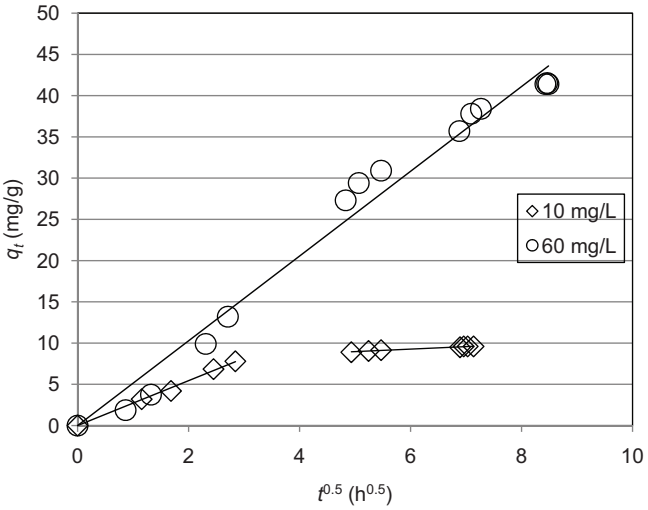

Fig. 7. Intraparticle diffusion model of methyl violet adsorption by MS.

4. Conclusion

Three sorbents were prepared from palm kernel shell and were used to test the adsorption of methyl violet dye of varying concentrations. FS displayed a higher specific surface area of 302 m^2/g, while KOH impregnation yields a sorbent rich in acidic oxygen functional groups. A 42 mg/g of methyl violet removal was recorded by MS, far better than that of

FS. The adsorption of methyl violet was mainly driven by chemical adsorption through the interaction between methyl violet molecules and acidic oxygen functional groups, while FS with superior specific surface area showed a positive effect on methyl violet removal compared with CS. The rate-limiting step for methyl violet switches from film diffusion to intraparticle diffusion as concentration increased. To conclude, a simple dried impregnation of palm kernel shell using potassium hydroxide is a promising sorbent candidate for methyl violet removal.

Acknowledgement

Financial support through UTM-Flagship No. 03G70 is greatly appreciated.

References

[1] A.A. Alqadami, Mu. Naushad, M.A. Abdalla, T. Ahmad, Z.A. Al-Othman, S.M. Al-Shehri, A.A. Ghfar, Efficient removal of toxic metal ions from wastewater using a recyclable nanocomposite: a study of adsorption parameters and interaction mechanism, J. Cleaner Prod., 156 (2017) 426–436.

[2] A.A. Alqadami, Mu. Naushad, M.A. Abdalla, M.R. Khan, Z.A. Al-Othman, Adsorptive removal of toxic dye using Fe_3O_4–TSC nanocomposite: equilibrium, kinetic, and thermodynamic studies, J. Chem. Eng. Data, 61 (2016) 3806–3813.

[3] E. Daneshvar, A. Vazirzadeh, A. Niazi, M. Kousha, Mu. Naushad, A. Bhatnagar, Desorption of methylene blue dye from brown macroalga: effects of operating parameters, isotherm study and kinetic modeling, J. Cleaner Prod., 152 (2017) 443–453.

[4] M. Naushad, M.R. Khan, Z.A. Al-Othman, M.R. Awual, A.A. Alqadami, Water purification using cost effective material prepared from agricultural waste: kinetics, isotherms and thermodynamic studies, CLEAN Soil, Air, Water, 44 (2016) 1036–1045.

[5] Mu. Naushad, M.R. Khan, Z.A. Al-Othman, I.H. Al-Sohaimi, F. Rodriguez-Reinoso, T.M. Turki, R. Ali, Removal of BrO_3^- from drinking water samples using newly developed agricultural waste-based activated carbon and its determination by ultra-performance liquid chromatography-mass spectrometry, Environ. Sci. Pollut. Res., 22 (2015) 15853–15865.

[6] T. Shu-Hui, M.A.A. Zaini, Dyes – Classification and effective removal techniques, In: J.C. Taylor, Advances in Chemistry Research, Vol. 30, Nova Science Publishers Inc., New York, 2016, pp. 19–34.

[7] R.M.M.D. Santos, R.G.L. Gonçalves, V.R.L. Constantino, C.V. Santilli, P.D. Borges, J. Tronto, F.G. Pinto, Adsorption of Acid Yellow 42 dye on calcined layered double hydroxide: effect of time, concentration, pH and temperature, Appl. Clay Sci., 140 (2017) 132–139.

[8] A.B. Albadarin, M.N. Collins, Mu. Naushad, S. Shirazian, Activated lignin-chitosan extruded blends for efficient adsorption of methylene blue, Chem. Eng. J., 307 (2017) 264–272.

[9] W. Chen, W. Lu, Y. Yao, M. Xu, Highly efficient decomposition of organic dyes by aqueous-fiber phase transfer and in situ catalytic oxidation using fiber-supported cobalt phthalocyanine, Environ. Sci. Technol., 41 (2007) 6240–6245.

[10] B. Shi, G. Li, D. Wang, C. Feng, H. Tang, Removal of direct dyes by coagulation: the performance of preformed polymeric aluminum species, J. Hazard. Mater., 143 (2007) 567–574.

[11] D. Mahanta, G. Madras, S. Radhakrishnan, S. Patil, Adsorption of sulfonated dyes by polyaniline emeraldine salt and its kinetics, J. Phys. Chem. B, 112 (2008) 10153–10157.

[12] D. Pathania, D. Gupta, A.H. Al-Muhtaseb, G. Sharma, A. Kumar, Mu. Naushad, T. Ahamad, S.M. Alshehri, Photocatalytic degradation of highly toxic dyes using chitosan-g-poly(acrylamide)/ZnS in presence of solar irradiation, J. Photochem. Photobiol., A, 329 (2016) 61–68.

[13] D. Pathania, R. Katwal, G. Sharma, Mu. Naushad, M.R. Khan, A.H. Al-Muhtaseb, Novel guar gum/Al_2O_3 nanocomposite as an effective photocatalyst for the degradation of malachite green dye, Int. J. Biol. Macromol., 87 (2016) 366–374.

[14] C.H. Tsai, J.D. Lin, C.H. Lin, Optimization of the separation of malachite green in water by capillary electrophoresis Raman spectroscopy (CE-RS) based on the stacking and sweeping modes, Talanta, 72 (2007) 368–372.

[15] L. An, J. Deng, L. Zhou, H. Li, F. Chen, H. Wang, Y. Liu, Simultaneous spectrophotometric determination of trace amount of malachite green and crystal violet in water after cloud point extraction using partial least squares regression, J. Hazard. Mater., 175 (2010) 883–888.

[16] M. Bahram, F. Keshvari, P. Najafi-Moghaddam, Development of cloud point extraction using pH-sensitive hydrogel for preconcentration and determination of malachite green, Talanta, 85 (2011) 891–896.

[17] D. Mahanta, G. Madras, S. Radhakrishnan, S. Patil, Adsorption and desorption kinetics of anionic dyes on doped polyaniline, J. Phys. Chem. B, 113 (2009) 2293–2299.

[18] G. Sharma, M. Naushad, A. Kumar, S. Rana, S. Sharma, A. Bhatnagar, F.J. Stadler, A.A. Ghfar, M.R. Khan, Efficient removal of coomassie brilliant blue R-250 dye using starch/poly(alginic acid-cl-acrylamide) nanohydrogel, Process Saf. Environ. Prot., 109 (2017) 301–310.

[19] C. Long, Z. Mai, Y. Yang, B. Zhu, X. Xu, L. Lu, X. Zou, Determination of multi-residue for malachite green, gentian violet and their metabolites in aquatic products by high-performance liquid chromatography coupled with molecularly imprinted solid-phase extraction, J. Chromatogr., A, 1216 (2009) 2275–2281.

[20] M.J.M. Bueno, S. Herrera, A. Uclés, A. Agüera, M.D. Hernando, O. Shimelis, M. Rudolfsson, A.R. Fernández-Alba, Determination of malachite green residues in fish using molecularly imprinted solid-phase extraction followed by liquid chromatography–linear ion trap mass spectrometry, Anal. Chim. Acta, 665 (2010) 47–54.

[21] S. Ming-Twang, L. Lin-Zhi, M.A.A. Zaini, Q. Zhi-Yong, A.Y. Pei-Yee, Activated carbon for dyes adsorption in aqueous solution, In: J.A. Daniels, Advances in Environmental Research, Vol. 36, Nova Science Publishers Inc., New York, 2015, pp. 217–234.

[22] L. Lin-Zhi, M.A.A. Zaini, Potassium carbonate-treated palm kernel shell adsorbent for congo red removal from water, J. Tek. (Sci. Eng.) 75 (2015) 233–239.

[23] Q. Zhi-Yong, M.A.A. Zaini, Adsorption of rhodamine B by palm kernel shell adsorbents, J. Eng. Tech., 7 (2016) 1–16.

[24] M.A.A. Zaini, T. Wee-Meng, M.J. Kamaruddin, S.H. Mohd-Setapar, M.A.C. Yunus, Microwave-induced zinc chloride activated palm kernel shell for dye removal, Sains Malaysiana, 43 (2014) 1421–1428.

[25] A.F. Rugayah, A.A. Aziz, N. Ngadi, Preparation and characterization of activated carbon from palm kernel shell by physical activation with steam, J. Oil Palm Res., 26 (2014) 251–264.

[26] A.R. Hidayu, N. Muda, Preparation and characterization of impregnated activated carbon from palm kernel shell and coconut shell for CO_2 capture, Procedia Eng., 148 (2016) 106–113.

[27] N.F. Jalani, A.A. Aziz, N.A. Wahab, W.H.W. Hassan, N.H. Zainal, Application of palm kernel shell activated carbon for the removal of pollutant and color in palm oil mill effluent treatment, J. Earth Environ. Health Sci., 2 (2016) 15–20.

[28] M.A.A. Zaini, K. Yoshihara, R. Okayama, M. Machida, H. Tatsumoto, Effect of out-gassing of $ZnCl_2$-activated cattle manure compost (CMC) on adsorptive removal of Cu(II) and Pb(II) ions, TANSO, 234 (2008) 220–226.

[29] M.A.A. Zaini, M. Zakaria, S.H. Mohd.-Setapar, M.A.C. Yunus, Sludge-adsorbents from palm oil mill effluent for methylene blue removal, J. Environ. Chem. Eng., 1 (2013) 1091–1098.

[30] M.A.A. Zaini, R. Okayama, M. Machida, Adsorption of aqueous metal ions on cattle-manure-compost based activated carbons, J. Hazard. Mater., 170 (2009) 1119–1124.

[31] R.K. Xu, S.C. Xiao, J.H. Yuan, A.Z. Zhao, Adsorption of methyl violet from aqueous solutions by the biochars derived from crop residues, Bioresour. Technol., 102 (2011) 10293–10298.

[32] M.A.A. Zaini, N. Alias, M.A.C. Yunus, Bio-polishing sludge adsorbents for dye removal, Pol. J. Chem. Technol., 18 (2016) 15–21.
[33] A. Saeid, H. Monireh, B. Hadis, Adsorption of methyl violet onto granular activated carbon: equilibrium, kinetics and modelling, Chem. Eng. J., 146 (2009) 36–41.
[34] M.A.A. Zaini, T.Y. Cher, M. Zakaria, M.J. Kamaruddin, S.H. Mohd.-Setapar, M.A.C. Yunus, Palm oil mill effluent sludge ash as adsorbent for methylene blue dye removal, Desal. Wat. Treat., 52 (2014) 3654–3662.
[35] Mu. Naushad, Z.A. Al-Othman, M.R. Awual, S.M. Alfadul, T. Ahamad, Adsorption of rose Bengal dye from aqueous solution by amberlite Ira-938 resin: kinetics, isotherms, and thermodynamic studies, Desal. Wat. Treat., 57 (2016) 13527–13533.
[36] Mu. Naushad, T. Ahamad, G. Sharma, M.M. Alam, Z.A. Al-Othman, S.M. Alshehri, A.A. Ghfar, Synthesis and characterization of a new starch/SnO_2 nanocomposite for efficient adsorption of toxic Hg^{2+} metal ion, Chem. Eng. J., 300 (2016) 306–316.